

A STRUCTURAL APPROACH TO JOINT INVERSION OF HYDROGEOPHYSICAL DATA

NIKLAS LINDE^{1,3}, ANDREW BINLEY², ARI TRYGGVASON³, LAUST B. PEDERSEN³,
ANDRÉ REVIL¹

¹ *Department of Hydrogeophysics and Porous Media, CNRS-CEREGE, Université Paul Cézanne, Europôle de l'Arbois, BP-80, 13545 Aix-en-Provence, France;*

² *Department of Environmental Science, Lancaster University, LA1 4YQ Lancaster, UK;*

³ *Department of Earth Sciences, Geophysics, Uppsala University, Villav. 16, 752 36 Uppsala, Sweden.*

ABSTRACT

We have developed a methodology to jointly invert electrical resistance tomography and radar traveltime data collected between boreholes. The models are coupled by enforcing structural similarity, which is obtained by keeping the cross-product of the gradients of the two models close to zero. The forward computations and the calculations of the Jacobians are performed with a finite element code for the electrical resistances and a finite difference traveltime algorithm for the traveltime data. The inverse problem is solved with LSQR where we maximize the amount of regularization for a given target data fit and a fixed weight that penalizes models where the cross-gradients function deviates from zero. An advantage of a structural approach to joint inversion is that petrophysical relationships can be evaluated *a posteriori*. A synthetic example illustrates that inversion artifacts can be reduced and that misplacement of anomalies can be partly avoided by the joint inversion. The inversion methodology could readily be adapted to a diverse set of applications in geophysics and hydrogeology.

1. INTRODUCTION

Geophysical methods are routinely utilized in hydrogeological studies, for example, to locate fault zones or to estimate the depth to a thick impermeable clay layer. One of the research goals in hydrogeophysics is to obtain, at a relevant scale and for a wide range of conditions, quantitative hydrogeological models from geophysical data. Two conditions must be fulfilled in order to reach this goal, namely: (1) reliable geophysical models and (2) reliable relationships between geophysical model parameters and relevant hydrogeological properties and state variables must be available. The first challenge is well-studied and purely geophysical, whereas the second challenge is truly multi-disciplinary involving geophysics, rock physics, and hydrogeology and is more poorly understood.

Improvements in geophysical models can be obtained by gathering more data of higher quality and by formulating inverse problems that are well adapted to the studied problem. However, different geophysical methods have different strengths and weaknesses, weaknesses that often prevail even if more data of higher quality are collected. For example, the diffusive nature of electrical methods makes it impossible to reconstruct sharp boundaries from electrical resistance tomography (ERT) data only and the resolution decreases with the

distance from the electrodes. To overcome these limitations, it is often necessary to introduce additional sources of information. Incorporation of *a priori* information is a useful way to incorporate downhole measurements in the inversion as well as introducing known interfaces. An alternative approach is to jointly invert different data types such that, for example, poorly constrained features in a model obtained from ERT data are also constrained by ground penetrating radar (GPR) data, and vice versa. The major problem with joint inversion is how to tie the different types of model parameters with each other as the underlying relationships are often unknown beforehand and are typically dependent on a multitude of rock properties and state variables.

We suggest that a structural approach to joint inversion is favorable in many geophysical applications (Haber and Oldenburg, 1997). The idea behind the structural approach is that spatial variations in geology are accompanied by changes in rock properties and state variables; different geophysical properties are thereby likely to change at the same location, but the changes might be of different magnitudes and possibly in different directions. Gallardo and Meju (2003) introduced the cross-gradients function, which is the cross-product of two different model vectors, to quantify structural similarity. Here we introduce an inversion method to jointly invert crosshole ERT and GPR data in three-dimensions while keeping the values of the cross-gradients function close to zero. The joint inversion method has the added advantage that the space-varying relationships between the different model types are obtained *a posteriori*, which is useful to understand petrophysical relationships and to obtain lithological zonations of the sub-surface.

This paper focuses on the validity of the assumptions underlying this approach to joint inversion of crosshole data and illustrates its applicability for a synthetic example. A detailed presentation of our joint inversion method and an application to unsaturated Sherwood Sandstone is presently under review (Linde et al., Joint inversion of crosshole electrical resistance and ground penetrating radar traveltimes data with application to unsaturated sandstone, *submitted to Water Resour. Res.*).

2. METHOD

2.1 Inversion method

Our inversion method is a regularized least-squares algorithm closely related to Occam's inversion (Constable et al., 1987), where a measure of model structure is minimized under the constraint that data misfit is below a given target misfit level.

Numerical solution of the ERT forward problem uses the Lancaster University 3D finite element code *R3*. Uniform resistivity is assigned within each linear brick type element in the finite element mesh. The model computes the voltage field resulting from point source current injection at each current electrode location. Computation of the voltage measurement for each four electrode configuration is then achieved using the principle of superposition. Calculation of the Jacobian is computed using the principle of reciprocity.

The forward modeling and computation of the Jacobian of the radar travel time data are based on the non-linear travel time tomography algorithm *PStomo_eq* (Tryggvason et al., 2002). The first arrival travel times are computed using the finite difference (FD) algorithm *time3d* of Podvin and Lecomte (1991), which is based on the first order approximation to the Eikonal equation. Ray tracing is performed by *a posteriori* back propagation perpendicular to the wave fronts from the receivers to the transmitters (Hole, 1992). The non-linearity of the

inverse problem of estimating the radar slowness (inverse of velocity) resides in that the ray paths depend on the slowness structure. Thus, if the slowness structure is changed, the ray paths will change as well. Therefore, new raypaths must be computed after each iteration. Assuming the slowness structure can be represented by cells of constant slowness, the elements in the Jacobian are simply the raylength in each cell.

In addition, we jointly invert the ERT and GPR travel time data by enforcing structural similarity, defined as models where the elements in the cross-gradients function is close to zero. The cross-gradients function at the previous iteration p at spatial location x , y , and z is defined as (Gallardo and Meju, 2003):

$$\mathbf{t}(x, y, z) = \nabla \mathbf{m}^\sigma(x, y, z) \times \nabla \mathbf{m}^s(x, y, z), \quad (1)$$

where \mathbf{m}^σ and \mathbf{m}^s are the models of the logarithm of electrical conductivity (S/m) and radar slowness (s/m), respectively. If the cross-gradients function is zero it implies that changes in the two models occur in the same or opposite direction or that the gradient of one of the models are zero for that element. The cross-gradients function is discretized using a forward difference scheme. The cross-gradients function for the present iteration is estimated by a first order Taylor expansion around the cross-gradients function at the previous iteration. The system of equations describing data misfit, model structure, and structural similarity are minimized in a least-square sense using the conjugate gradient algorithm LSQR (Paige and Saunders, 1982). An iterative solution of the systems of equations is suitable because we want to solve 3D problems where computer memory is a limiting factor. The sparseness of the systems of equations is utilized by using sparse solvers.

In a first stage, we perform separate inversions of the ERT and the GPR travel time data to determine a constant standard deviation of the data for which solutions with a weighted root mean square (RMS) of 1 can be found and where the standard deviations are equal or higher than the estimated errors of the data. This procedure ensures an even weighting of the two data types. If the underlying resistivity and slowness structure are structurally similar, a weighted RMS of 1 should also be reached for the models derived from the joint inversion.

2.2 Petrophysical justification of inversion method

It is possible to perform joint inversion by minimizing the cross-gradients function without considering the possible relationships between the underlying physical properties (Gallardo and Meju, 2004). However, minimization of the cross-gradients function is not recommended for several types of applications and conditions. To exemplify the validity of our inversion method, we consider a partially saturated sand/siltstone and the expected relationships between relative permittivity and electrical conductivity in such a system. We used the inverse of the electrical formation factor instead of porosity when deriving the volume averaging equations. The inverse of the electrical formation factor is a good estimate of effective porosity (e.g., Revil et al., 1998).

The effective relative permittivity, κ_{eff} , is given by

$$\kappa_{eff} = \frac{1}{F} \left[S_w^n \kappa_w + (1 - S_w^n) \kappa_a + (F - 1) \kappa_s \right], \quad (2)$$

where κ_w , κ_a , and κ_s are the relative permittivities of water, air, and the minerals forming the rock matrix, respectively; $F = \phi^{-m}$ is the electrical formation factor (where ϕ is the interconnected porosity and m is Archie's first exponent), S_w is the water content, and n is

Archie's second exponent (e.g., Waxman and Smits, 1968). In the following, we adopt the common practice of assuming that κ_w , κ_a , and κ_s are constant within the volume of interest.

The electrical conductivity of the air and the mineral grains are neglected, but surface conduction can be significant (e.g., Revil and Glover, 1998). The resulting equation for electrical conductivity reads

$$\sigma_{eff} = \frac{1}{F} [S_w^n \sigma_w + (F - 1) \sigma_s], \quad (3)$$

where σ_{eff} (S/m) is the effective electrical conductivity of the media, σ_w (S/m) is the electrical conductivity of the pore water and σ_s (S/m) is the surface conduction. Eq. (3) is reduced to Archie's law when surface conductivity can be neglected. For a granular material with uniform grain radius R (m), the surface conductivity entering Eq. 3 is

$$\sigma_s = \frac{2}{R} \Sigma_s, \quad (4)$$

where Σ_s (S) is the specific surface conductivity and is fairly constant in comparison with R (e.g., Leroy and Revil, 2004). For non-uniform grain distributions it is necessary to replace R with an effective grain radius R_{eff} (m).

2.2.1 Saturated media

In saturated media, Eqs. 2-3 simplify to

$$\kappa_{eff} = \frac{1}{F} [\kappa_w + (F - 1) \kappa_s], \text{ and} \quad (5)$$

$$\sigma_{eff} = \frac{1}{F} [\sigma_w + (F - 1) \sigma_s] \quad (6)$$

Variations in κ_{eff} are only affected by variations in F , whereas variations in σ_{eff} can be attributed to variations in either F , σ_w , or σ_s . Minimization of the cross-gradients function (see Eq. 1) is for a random media only valid if σ_s and σ_w are strongly correlated with F or if σ_s can be neglected or assumed to be constant and σ_w is constant. If these conditions are not fulfilled it is necessary to consider the earth structure to be composed of fairly homogeneous zones, where any variations in rock properties from one zone to another occurs at the same location if they change, which is the justification for the method presented by Gallardo and Meju (2003). This is a reasonable assumption when the sub-surface consists of fairly distinct units, but is not valid for materials that are better described as continuous random fields, in that case, imposing that the cross-gradients function is close to zero will remove small scale features. Minimization of the cross-gradients function is clearly inappropriate in applications where variations of σ_w is varying gradually in a different direction compared with the normal of geological boundaries, which would be expected at contaminated sites.

2.2.2 Unsaturated media

In unsaturated media, the problem is further complicated by S_w^n and minimizing the cross-gradients function is meaningful only if the gradients of S_w^n are normal to geological boundaries or if changes in S_w^n is confined within fairly homogeneous geological units. The same reasoning applies both to σ_w or σ_s . However, the electrical formation factor can vary freely.

3. A SYNTHETIC EXAMPLE

A simplified two-dimensional electrical resistivity (Figure 1a) and radar velocity model (Figure 1d) is used to illustrate the advantages of joint inversion by minimizing the cross-gradients function. Two anomalies are immersed into uniform background models. The parameters used to calculate κ_{eff} (see Eq. 5) and σ_{eff} (see Eq. 6) represent typical values for saturated shales and sandstones (Table 1). Radar velocity, v (m/s), is related to κ_{eff} as $\kappa_{eff}=c^2/v^2$, where c is the speed of light ($\cong 3 \times 10^8$ m/s).

TABLE 1: Rock properties of the synthetic model.

	Background	Upper anomaly	Lower anomaly
ϕ	0.3	0.356	0.3
m	1.8	2.1	2.1
S_w^n	1	1	1
κ_w	81	81	81
κ_s	5	5	5
σ_w (S/m)	0.0769	0.0769	0.0769
σ_s (S/m)	0	0.4	0.4
<i>Resulting parameters</i>			
F	8.73	8.75	12.53
κ_{eff}	13.7	13.7	11.1
σ_{eff} (S/m)	0.00881	0.0442	0.0429

A hypothetical ERT survey yielding 760 measurements was performed by placing electrodes with 1 m spacing in two hypothetical boreholes and by contaminating the calculated response by Gaussian noise assuming a relative error of 5%. A hypothetical crosshole multiple-offset gather GPR survey with 0.25 m spacing between the same boreholes resulted in 1312 radar traveltimes, which were contaminated by Gaussian errors of magnitude 0.1 ns. The individual ERT inversion converged to the weighted RMS target misfit of 1 after 3 iterations starting from 28.2 (Figure 1b). The resulting model is accurate in modeling transitions in the vertical direction, but the accuracy in the horizontal direction is very poor illustrating a non-unique inverse problem. The resulting models could be much improved by employing surface based electrodes as well as using a different survey configuration, but the example illustrates the common problem of non-uniqueness. Can joint inversion with GPR travel time data improve the ERT models? The individual GPR inversion converged to the weighted RMS target misfit of 1 after 8 iterations starting from 25 (Figure 1e). The resulting radar velocity model is a good representation of the true radar velocity, even if the low relative permittivity anomaly has a too high relative permittivity and the smoothness regularization makes the interface with the background difficult to define. Inversion artifacts are also present at the top corners of the tomogram. Can joint inversion with ERT data decrease the artifacts and improve the imaging of the relative permittivity anomaly?

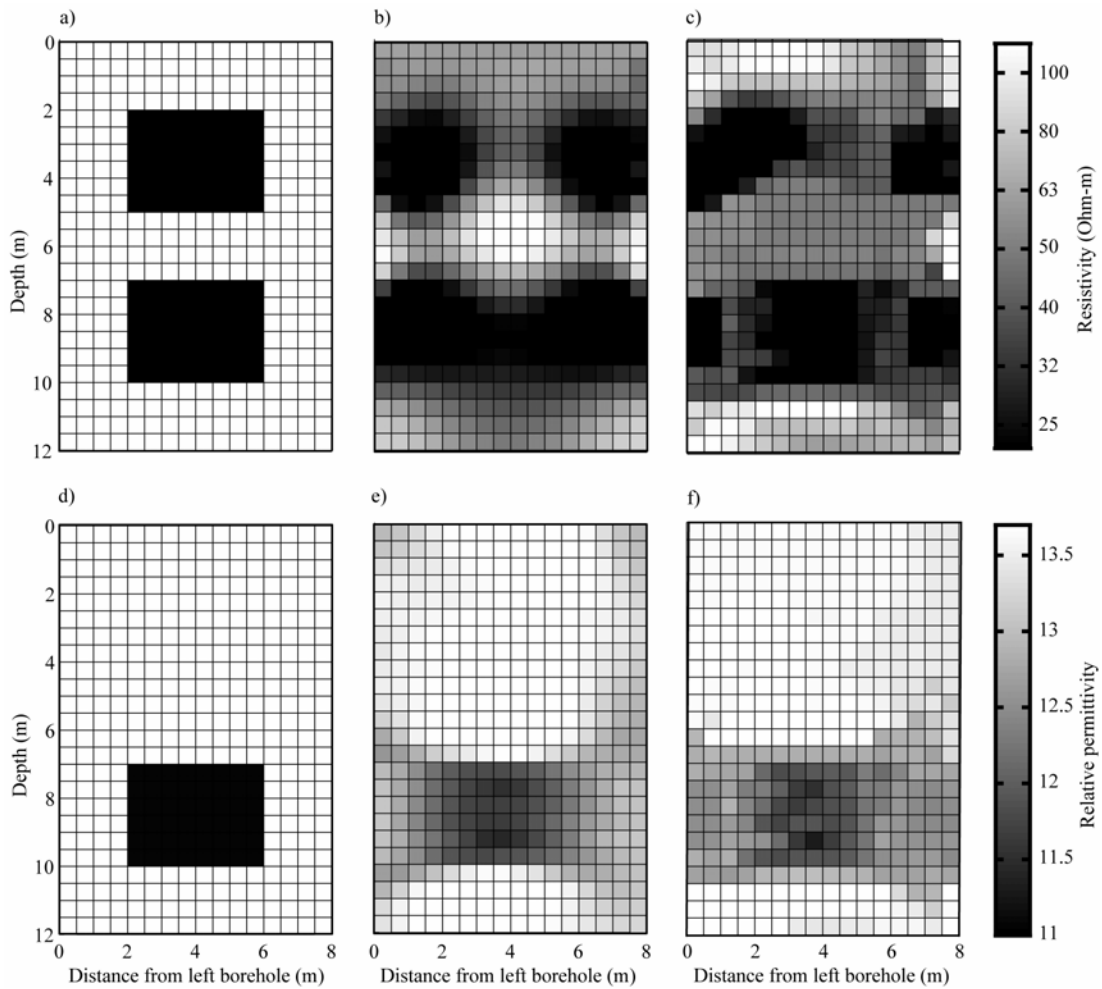


FIGURE 1. True electrical resistivity model (a), electrical resistivity model based on individual inversion (b), electrical resistivity model based on joint inversion (c). True relative permittivity model (d), relative permittivity model based on individual inversion (e), relative permittivity model based on joint inversion (f).

The joint inversion reached a weighted RMS data misfits of 1.4 for the electrical resistances (Figure 1c) and 1.8 for the radar traveltimes (Figure 1f) after ten iterations. The resistivity model has the lower anomaly accurately placed, even though false low resistivity zones are still found close to the boreholes. The relative permittivity model has no longer any inversion artifacts at the top of the tomogram. These artifacts did not improve the data fit significantly and they consequently disappeared when performing the joint inversion.

Scatter plots between relative permittivity and electrical resistivity based on the individual (Figure 2a) and the joint inversions (Figure 2b) reveal much less scatter in the models based on the joint inversion. For the joint inversion, the model values corresponding to the low relative permittivity zone fall on a straight line that approximately approaches the true values. The value for the cross-gradients function for the individually (Figure 2c) and jointly inverted models (Figure 2d) reveal that the cross-gradients function deviates significantly from zero for the individual inversions and that it is more than ten times lower for the jointly inverted models.

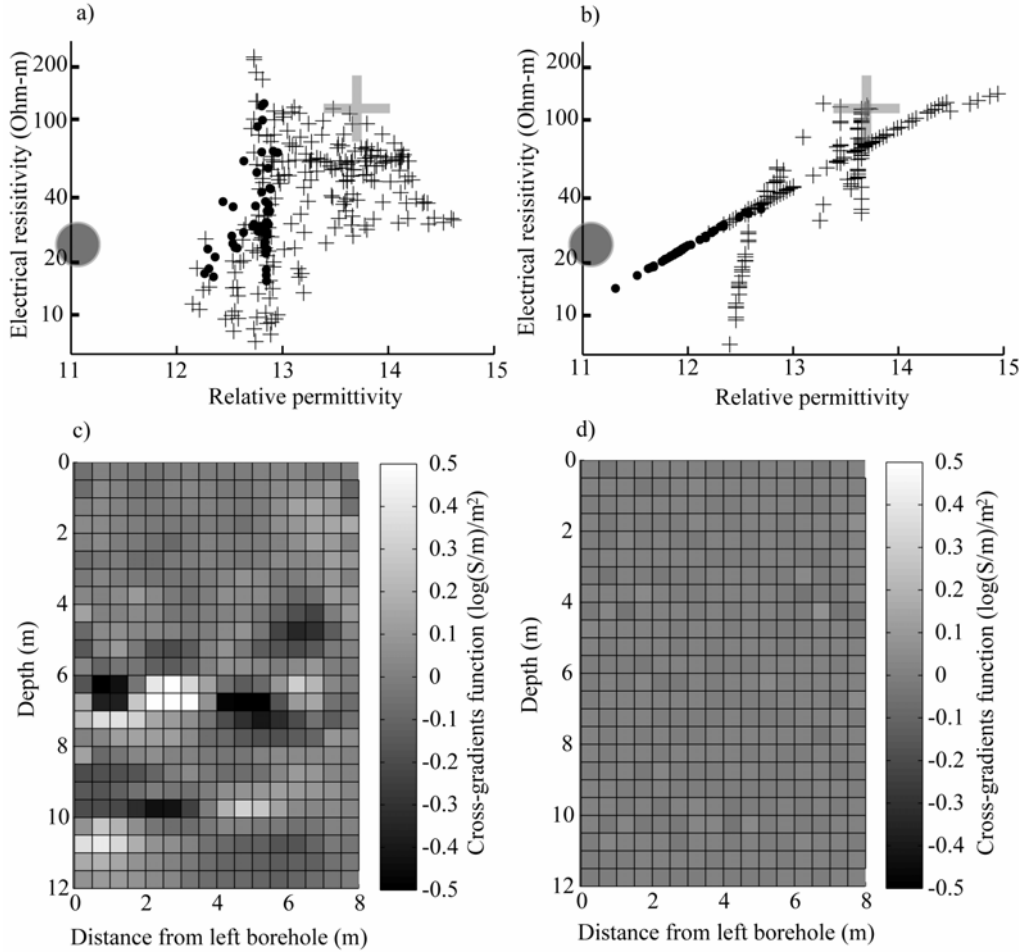


FIGURE 2. Scatter plots of electrical resistivity vs. κ_{eff} for the individual inversion models (a), as well as for the joint inversion models (b). Note the large grey symbols that indicate the corresponding values for the underlying true model. The cross-gradients function for the individual inversions (c) and the much lower cross-gradients function for the joint inversion (d) illustrate that the joint inversion algorithm enforces structural similarity.

4. DISCUSSION AND CONCLUSIONS

Joint inversions realized by minimizing the cross-gradients function have been successfully applied to jointly invert seismic refraction and surface-based ERT data in two dimensions (Gallardo and Meju, 2003; 2004); to perform local earthquake (LE) tomography with joint inversion for P- and S-wave velocities in three dimensions (Tryggvason and Linde, 2006); to jointly invert crosshole ERT and GPR traveltime data in three dimensions (Linde et al., submitted). In order to be computationally feasible, three-dimensional applications should preferably employ iterative solvers (such as LSQR) that utilize the sparseness of the systems of equations to be solved. Two-dimensional inversions should only be performed when the assumptions of a two-dimensional earth structure is reasonably valid as different geophysical methods have different sensitivities to three-dimensional heterogeneities. Performing joint two-dimensional inversion when the sub-surface is highly three-dimensional is likely to produce significant ghost features. The structural approach is strictly valid only when both

model properties primarily depend on the same rock property (e.g., the electrical formation factor). However, minimization of the cross-gradients function is often a good approach when variations in the geological structure are fairly distinct and when there are insignificant variations in state variables. Otherwise, it is necessary to carefully assess the validity of minimizing the cross-gradients function for the methods used and the problem at hand using petrophysical models (see Section 2) or, at least, by comparing the resulting models with those obtained from individual inversions.

In hydrogeophysics, the target is often state variables such as S_w or σ_w that are often studied using time-lapse measurements where geological structure cancels in the resulting images. Joint inversions based on the cross-gradients function appear ideal in such applications.

Even if not addressed here, we believe that a structural approach to joint inversion is well-suited to jointly invert hydraulic head and tracer test data together with different types of geophysical data. For example, joint inversion of tracer test and crosshole GPR traveltimes data based on a structural approach is likely to improve models of hydraulic conductivity compared with sequential approaches (e.g., Linde et al., 2006).

5. ACKNOWLEDGEMENTS

This research was supported, in part, by the Swedish Geological Survey under contract No. 60-1307/2004.

REFERENCES

- Constable, S. C., R. L. Parker, and C. G. Constable (1987), Occams inversion – a practical algorithm for generating smooth models from electromagnetic sounding data, *Geophysics*, 52 (3), 289-300.
- Gallardo, L. A., and M. A. Meju, (2003), Characterization of heterogeneous near-surface materials by joint 2D inversion of dc resistivity and seismic data, *Geophys. Res. Lett.*, 30 (13), 1658.
- Gallardo, L. A., and M. A. Meju (2004), Joint two-dimensional DC resistivity and seismic travel time inversion with cross-gradient constraints, *J. Geophys. Res.*, 109, B03311, doi: 10.1029/2003JB002716.
- Haber E, and D. Oldenburg (1997), Joint inversion: A structural approach, *Inverse probl.*, 13(1), 63-77.
- Hole, J. A. (1992), Nonlinear high-resolution three-dimensional seismic travel time tomography, *J. Geophys. Res.*, 97 (B5), 6553-6562.
- Linde, N., S. Finterle, S. Hubbard (2006), Inversion of tracer test data using tomographic constraints, *Water Resour. Res.*, *accepted*.
- Paige, C. C., and M. A. Saunders (1982), LSQR: An algorithm for sparse linear equations and sparse least squares, *ACM Trans. Math. Software*, 8 (1), 43-71.
- Podvin, P., and I. Lecomte (1991), Finite difference computation of travel times in very contrasted velocity models: A massively parallel approach and its associated tools, *Geophys. J. Int.*, 105 (1), 271-284.
- Revil, A., and P. J. Glover (1998), Nature of surface electrical conductivity in natural sands, sandstones, and clays, *Geophys. Res. Lett.*, 25 (5), 691-694.
- Revil, P., and A. Revil (2004), A triple-layer model of the surface electrochemical properties of clay minerals, *J. Colloid Interf. Sci.*, 270 (2), 371-380.
- Tryggvason, A., S. Th. Rögnvaldsson, and Ó. G. Flovenz (2002), Three-dimensional imaging of the P- and S-wave velocity structure and earthquake locations beneath Southwest Iceland, *Geophys. J. Int.*, 151 (3), 848-866.
- Tryggvason, A., and N. Linde (2006), Local earthquake (LE) tomography with joint inversion for P- and S-wave velocities using structural constraints, *Geophys. Res. Lett.*, *accepted*.
- Waxman, M. H., and L. J. M. Smits (1968), Electrical conductivities in oil-bearing shaly sands, *Soc. Pet. Eng. J.*, 8, 107-122.